Research Square

Preprints are preliminary reports that have not undergone peer review.
They should not be considered conclusive, used to inform clinical practice,
or referenced by the media as validated information.

Role of slow temporal dynamics in the reliable activity of stochastically driven neurons

Subhadra Mokashe
Yale University
Suhita Nadkarni
suhita@iiserpune.ac.in

Indian Institute of Science Education and Research, Pune

Research Article

Keywords: stochasticity, regular rhythmic activity, CPG, Gillespie algorithm, extrinsic noise, intrinsic noise, reliability 1

Posted Date: October 5th, 2026

DOI: https://doi.org/10.21203/rs.3.rs-10945064/v1

License: This work is licensed under a Creative Commons Attribution 4.0 International License.
Read Full License

Additional Declarations: No competing interests reported.

Role of slow temporal dynamics in the reliable activity of stochastically driven neurons

Subhadra Mokashe[1,2] and Suhita Nadkarni[2*]

[1]Department of Neuroscience, Yale University, 100 College Street, New Haven, 06510, Connecticut, United States of America.
[2*]Department of Biology, Indian Institute of Science Education and Research, Pune, Dr. Homi Bhabha Road, Pune, 411008, Maharashtra, India.

*Corresponding author(s). E-mail(s): suhita@iiserpune.ac.in;
Contributing authors: subhadramokashe@gmail.com;

Abstract

Neuronal networks maintain robust patterns of activity despite a backdrop of noise from various sources. Mutually inhibiting neurons is a standard network motif implicated in rhythm generation. In a 'building-block' network motif of two mutually inhibiting neurons capable of swapping from an active state to a quiescent state, we ask how different sources of stochasticity alter firing patterns. In this system, the alternating activity occurs via the combined action of a calcium-dependent potassium current, sAHP (slow afterhyperpolarization), and a fast GABAergic synapse. We show that one of the payoffs of extrinsic noise is extending the dynamical range of neuronal firing. Extrinsic noise also has the effect of increasing the switching frequency via a faster build-up of sAHP current. The switching frequency as a function of input current has a non-monotonic behavior. Interestingly, the noise tolerance of this system varies with the input current. It shows maximum robustness to noise at an input current that corresponds to the minimum switching frequency between the neurons. The slow decay time scale of sAHP conductance allows neurons to act as a low-pass filter, attenuates noise, and integrates over ion channel fluctuations. We also show that the slow inactivation time of the sAHP channel allows the neuron to act as an action potential counter. We propose that in this system, the slow decay time scale of sAHP conductance, an intrinsic property of the current, allows the network to maintain robust rhythmic activity critical for various functions despite noise.

Keywords: stochasticity, regular rhythmic activity, CPG, Gillespie algorithm, extrinsic noise, intrinsic noise, reliability

1 Introduction

Several key brain functions critically depend on the reliable activity of neuronal networks. One of the enduring questions in neuroscience has been to understand how neurons generate robust activity patterns despite an inherently noisy framework. Here, we ask how noise arising from intrinsic sources, such as thermal fluctuations in ion channels, and extrinsic sources, such as a variable input, affect activity in an illustrative network capable of generating rhythms. The network consists of two neurons connected by an inhibitory fast GABAergic synapse that causes post-synaptic neurons to switch off as synaptic current builds up (See Figure 2). Mutually inhibitory networks of neurons are a recurring motif across brain areas, for example, in the hippocampus [1], central pattern generators associated with locomotion and digestion [2], insect olfactory systems [3], REM sleep cycle [4], and working memory [5]. The on-off switching activity of neurons allows them to be associated with multiple networks [6]. It also dictates the sequential order of activity required, for example, locomotion [7] and spatial navigation [8].

Effects of various sources of noise on system behavior and, generally, on brain function have been extensively investigated [9, 10]. Noise can be both disruptive and enhance function [11]. The addition of noise can increase signal detection and transduction via stochastic resonance in Hippocampal CA1 neurons. [11–13]. Coherence resonance is another interesting phenomenon that arises due to noise but increases the regularity of activity [14]. Apart from these external sources of noise (extrinsic noise), intrinsic sources of variability such as channel fluctuations can also modify function [13]. Noisy opening of voltage-gated calcium channels can allow intracellular calcium influx and trigger downstream calcium-mediated signals, make the neuron more excitable, allow transmission of subthreshold signals [15], and cause a post-inhibitory rebound effect [16].

In our model, the effect of extrinsic noise is studied by varying the amplitude of the noise of the input current. It has been shown that the voltage-gated calcium channel (VGCC) fluctuations are one of the main contributors to the stochasticity at the synapse [17]. We study the influence of intrinsic noise arising from channel fluctuations of the VGCCs on our two-neuron rhythm-generating network.

2 Methods

We used an ionic conductance-based model of neurons that are connected via inhibitory synapses. The potassium current, sAHP (slow afterhyperpolarization), which is mediated by calcium ions, orchestrates switching in the network (equations (1), (2)). Extrinsic noise is interpreted as the noise arising independently of the state of the neuron, such as the background noise, and is implemented here as an additive term ξ to the differential equation of the voltage (equations (1), (2)). In contrast, intrinsic noise depends on the state of the neuron. It is implemented in the model as the stochasticity associated with a small number of ion channels and stochastic channel opening. To model realistic intrinsic noise, we simulate a Markovian description of the calcium channels using a modified Gillespie algorithm.

2.1 Network model

The neurons have voltage-gated calcium channels, and sAHP channels along with voltage-gated sodium and potassium channels leak current and extrinsic noise (gaussian white noise (ξ) $\sim \mathcal{N}(0,1)$).

$$C\frac{dV_1}{dt} = I_{external} - I_{Na} - I_K - I_{Leak} - I_{synapse} - I_{VGCC} - I_{sAHP} + \text{noise amplitude } \xi_1 \tag{1}$$

$$C\frac{dV_2}{dt} = I_{external} - I_{Na} - I_K - I_{Leak} - I_{synapse} - I_{VGCC} - I_{sAHP} + \text{noise amplitude } \xi_2 \tag{2}$$

2.2 Hodgkin-Huxley Neuron Model

The classical Hodgkin-Huxley neuron model describes how neurons generate action potentials [18]. The neuron model has Na^+, K^+, and leak channels and the dynamics are given by the following system of equations:

$$C\frac{dV}{dt} = -\bar{g}_{Na}m^3h(V - E_{Na}) - \bar{g}_K n^4(V - E_K) - g_L(V - E_L) + I \tag{3}$$

$$\frac{dx}{dt} = \alpha_x(1 - x) - \beta_x x \quad \text{where, } x = n, m, h \tag{4}$$

Where,
V: membrane potential
n, m, h: gating variables which represent the open fraction of channels of sodium (m, h) and potassium(n).
C = 1 μF/cm^2: the capacitance of the cell membrane
E_{Na} = 50 mV, E_K = -77 mV, and E_L = -54.4 mV: reversal potentials of sodium, potassium and leak channels respectively.
$\bar{g}_{Na}$ = 120 mS/cm^2 and $\bar{g}_K$ = 36 mS/cm^2: maximal conductances of sodium and potassium currents respectively.
g_L = 0.3 mS/cm^2: leak conductance

$$\alpha_m = \frac{.1(V + 40)}{1 - exp(-.1(V + 40))} \tag{5}$$

$$\beta_m = 4.0exp(-(V + 65)/18.0) \tag{6}$$

$$\alpha_h = .07exp(-(V + 65)/20.0) \tag{7}$$

$$\beta_h = \frac{1}{1 + exp(-(V + 35)/10)} \tag{8}$$

$$\alpha_n = \frac{.01(V + 55)}{1 - exp(-(V + 55)/10)} \tag{9}$$

$$\beta_n = 0.125exp(-(V + 65)/80.0) \tag{10}$$

$$I_{Na} = g_{Na}m^3h(V - E_{Na}) \tag{11}$$

$$I_K = g_K n^4 (V - E_K) \tag{12}$$
$$I_{Leak} = g_{leak}(V - E_{Leak}) \tag{13}$$

2.3 sAHP channels

The model for calcium-mediated potassium current, sAHP is based on the sAHP channels of CA1 pyramidal neurons [19] [20].

$$R \underset{r_u}{\overset{4r_b}{\rightleftharpoons}} CaR \underset{2r_u}{\overset{3r_b}{\rightleftharpoons}} 2CaR \underset{3r_u}{\overset{2r_b}{\rightleftharpoons}} 3CaR \underset{4r_u}{\overset{r_b}{\rightleftharpoons}} 4CaR \underset{r_c}{\overset{r_o}{\rightleftharpoons}} O \tag{14}$$

Where $r_b = 4\ 10^6 M^{-1} sec^{-1}$, $r_u = 0.5$/sec, $r_o = 600$/sec , and $r_c = 400$/sec. Here R, CA1R, CA2R, CA3R, CA4R, and O are the states of the channel. R is the closed state, and O is the open state. The total conductance of the channel is dependent on the fraction of open channels. The peak open probability of the channel is 0.4, and its mean open time is 2.5 msec. When $[Ca^{2+}]_i$ falls rapidly, the decay of sAHP is limited by the channel closing and Ca^{+2} dissociation rates to give a time constant of 1.5 sec [19].

$$I_{sAHP} = g_{sAHP} \frac{N_O}{N_t} (V - E_{sAHP}) \tag{15}$$

Here $g_{sAHP} = 0.4$ mS/cm^2 and $E_{sAHP} = E_K =$ -77 mV, N_O/N_t is the fraction of channels in the open state.

2.4 Synapse

Inhibitory synapses are modelled using a tan hyperbolic function.

$$\rho = \frac{1 + tanh(\frac{V}{4})}{2} \tag{16}$$

$$\frac{ds}{dt} = \frac{\rho}{\tau_r}(1 - s) - \frac{1}{\tau_d} s \tag{17}$$
$$I_{syn} = \bar{g}_{syn} s (V - E_{syn}) \tag{18}$$

Where $\bar{g}_{syn} = 2.2\ mS/cm^2$, $E_{syn} =$ - 80 mV, $\tau_r = 0.3\ msec$ and $\tau_d = 8.9\ msec$.

2.5 Voltage gated calcium channels

We model the L-type $CaV_{1.3}$ calcium channels which open at low voltages given by [20].

$$S_0 \underset{\beta(V)}{\overset{2\alpha(V)}{\rightleftharpoons}} S_1 \underset{2\beta(V)}{\overset{\alpha(V)}{\rightleftharpoons}} S_2 \tag{19}$$

$$\alpha(V) = \frac{\sqrt{x_\infty}}{\tau} \tag{20}$$

$$\beta(V) = \frac{1 - \sqrt{x_\infty}}{\tau} \tag{21}$$

$$x_\infty(V[mV]) = \frac{1}{1 + e^{-\frac{(V+30)}{6}}} \tag{22}$$

Here $\alpha(V), \beta(V)$ are voltage dependent probabilities of transitions of states S_i . The conductance is dependent on the fraction of open state N_{S_2}/N_t .

$$I_{CaV} = g_{CaV} \frac{N_{S_2}}{N_t}(V - E_{CaV}) \tag{23}$$

Here $g_{CaV} = 0.15$ mS/cm^2 , $\tau = 2.5$msec, and $E_{CaV} = E_{Ca} = 25$ mV.

2.6 Modelling calcium dynamics

The intracellular calcium concentration dynamics is modeled as a leaky integrator, [20, 21].

$$\frac{d[Ca^{2+}]}{dt} = (-\alpha_{Ca} I_{CaV}) - \frac{([Ca^{2+}])}{\tau_{Ca}} \tag{24}$$

Where $\alpha_{Ca} = 2{\times}10^{-4}[mM(msec\mu A)^{-1}cm^2]$ and $\tau_{Ca} = 14$ ms. α_{Ca} depends on the area-to-volume ratio of the neuron, intracellular buffering of calcium, and stochasticity factor and converts calcium current into the units of calcium concentration per unit of time. At the resting voltage, the calcium concentration is 100 nM and goes up to 2.5 μM during a spike.

2.7 Calcium channel opening failures

To test how sAHP integrates over the irregular and unreliable calcium signal, we induce calcium channel opening failures with a given probability. Calcium failures are modeled as pulse failures, where none of the calcium channels open. Each calcium pulse can be missed by sAHP current with a certain probability (failure rate). The pulse failure is limited to the duration of the calcium pulse and is carried out by multiplying a voltage-dependent block on the calcium current (equation 23). The calcium current rises again after the failed calcium pulse due to the rise in voltage.

2.8 Modelling channel noise

For a large number of ion channels, the fluctuations in the total conductance are small and can be modeled using deterministic dynamics. However, a small number of ion channels typically dictate neuronal dynamics. Under these circumstances, the stochasticity of ion channel fluctuations becomes relevant. Various methods to model channel noise have been explored and reviewed in [9]. Stochastic dynamics are simulated using

the Gillespie algorithm, which is a fast and accurate algorithm to simulate channel noise [22].

Given that the fluctuations arising from VGCCs are significant contributors to noise in the calcium signal that ultimately governs switching dynamics, we selectively target the investigation of noise arising from calcium channel fluctuations. Towards this control experiment, we implement a Markovian description of only VGCCs using the Gillespie algorithm [22], whereas the other components of the model are modeled deterministically. To accurately capture all transitions, we developed an algorithm to implement the Gillespie algorithm (for Markovian progression) and the Euler method (for deterministic progression) "in tandem" for a system of equations with multiple timescales that span several orders of magnitude ([20] (slowAHP $\tau = 1.5$ s, fast voltage, and calcium dynamics τ=14 ms). We call this Gillespie-Euler Hybrid Algorithm the 'Tandem Progression Gillespie' (TPG), which is used to simulate realistic time scales and amplitudes of channel noise.

In our implementation of the Gillespie Algorithm, we updated the entire system at 1) the fixed time step dictated by the deterministic part of the model and 2) the waiting times obtained from modeling the calcium channel dynamics as a Poisson process. This implementation is distinct from [23], where the voltage is updated only at times dictated by channel transitions. This modification was crucial as the build-up of sAHP due to calcium fluctuations would otherwise be missed between the channel waiting times. This would be especially true when the waiting times are longer. Thus, by updating the whole system together at a time that arises either out of the calcium channel fluctuations or the voltage equations, the dynamics of this multi-timescale system evolved more accurately via TPG.

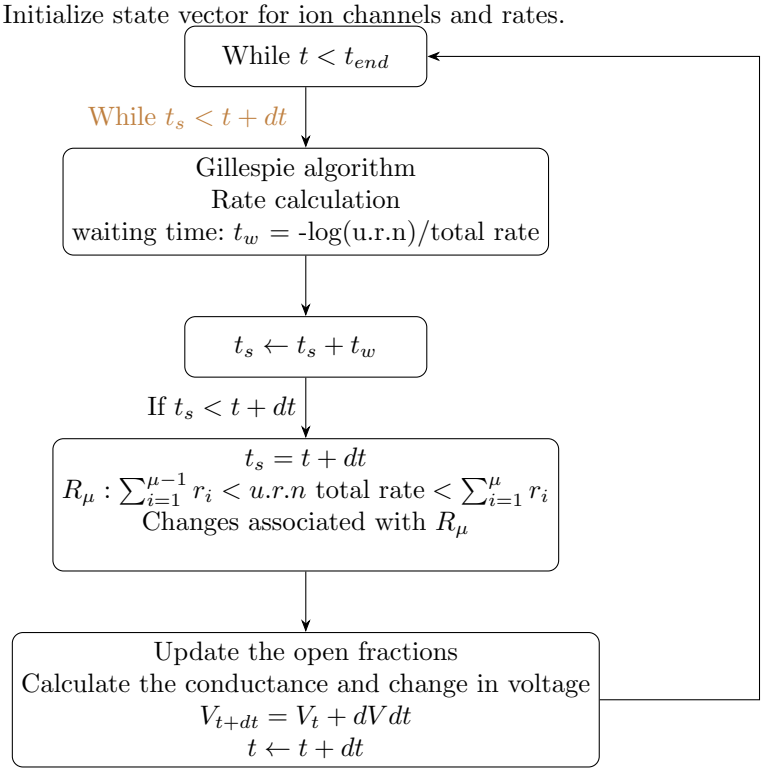
In the algorithm by Goldwyn et al. [9] (Model DB accession number 138950), voltages are updated at a fixed time step. This algorithm is correct under the assumption that 1) the rates for transitions do not change between the two time steps and 2) there are no slow timescales involved that could keep track of all the fluctuations, as the fluctuations between the fixed time steps may not be seen by the voltage and other currents in the neuron.

Another implementation of the Gillespie algorithm for conductance-based neurons suggested by Chow et al. [23] integrates the deterministic system till the waiting time given by the Gillespie algorithm and updates the stochastic system only after Gillespie waiting times. This algorithm assumes that the rate constants do not change during the time step, and the rate and waiting time calculations take into account the dynamics and time scales from all the ion channels present in the neuron.

To isolate the influence of noise due to VGCC fluctuations, we use the Markovian kinetic scheme to simulate channel dynamics, whereas the rest of the system is allowed to evolve deterministically. Since we wanted to study the effect of the channel noise arising from one type of ion channel, these modifications were essential. Integrating at fixed time steps as in [9] will lead to missing channel fluctuations that take place between two time steps. The fast activation and slow decay timescales associated with the sAHP current will cause the fluctuations caused by a noisy current input to have a cumulative effect on the sAHP current and significantly modify switching times between neurons. To not miss these fluctuations, we update the whole system

Algorithm 1 Goldwyn and Shea-Brown Gillespie Modification

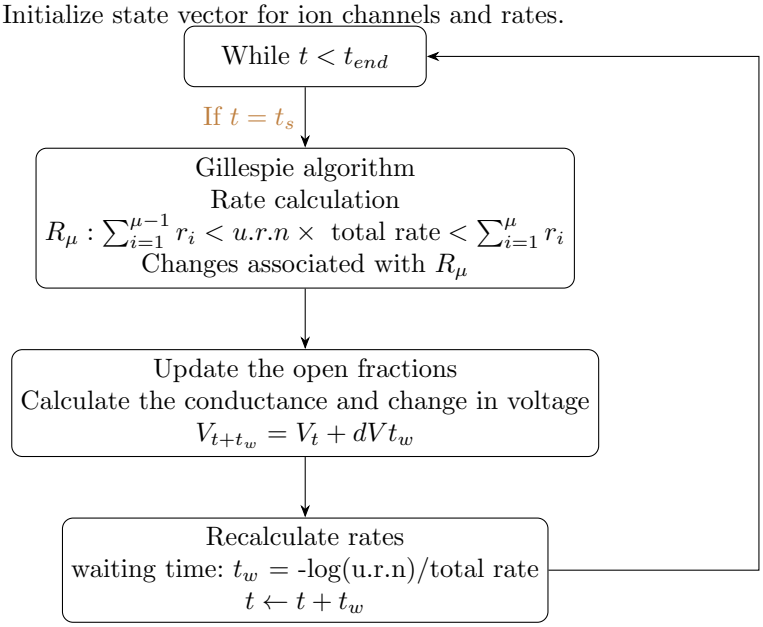
$t_s \leftarrow$ time of the next transition,
$t_w \leftarrow$ time to the next transition,
$dt \leftarrow$ fixed time step,
$u.r.n \leftarrow$ uniform random number,
Initialize state vector for ion channels and rates.



deterministically, and in 'tandem,' the stochastic system at the Gillespie algorithm-determined time steps. While integrating merely at long waiting times associated with small channel numbers, the dynamics of the other components of the model neuron may not be captured correctly and could lead to errors. To model the neuronal dynamics correctly, especially when the waiting times are longer than a fixed time step (0.01 msec used in simulations), we integrate the system at the fixed time step and also update the stochastic channel states at every integration step to take into account the changed voltage and current values. Thus, by updating the whole system together, we believe that we are modeling the stochastic channel dynamics as well as the neuronal and network dynamics accurately. In summary, in Tandem Progression Gillespie, every component of the model is updated at the same time and is described in Algorithm 3. Unlike fast Markovian channel noise methods, which focus primarily on computational efficiency [24], TPG is designed specifically to handle the multi-timescale coupling

Algorithm 2 Chow and White Gillespie Modification

$t_s \leftarrow$ time of the next transition,
$t_w \leftarrow$ time to the next transition,
$t \leftarrow$ current time,
$u.r.n \leftarrow$ uniform random number,
Initialize state vector for ion channels and rates.



between stochastic channel dynamics, slow conductances, and stochastic synaptic and network dynamics [25, 26].

For higher channel numbers, the Chow and White and TPG algorithms show similar trends in switching, see in Figure 1 as most transitions occur at the Gillespie waiting time.

2.9 insilico

insilico is a C++-based computational tool specifically designed and developed to simulate neurons. The deterministic model is implemented using insilico-0.25 http://www.iiserpune.ac.in/∼collins/insilico/.

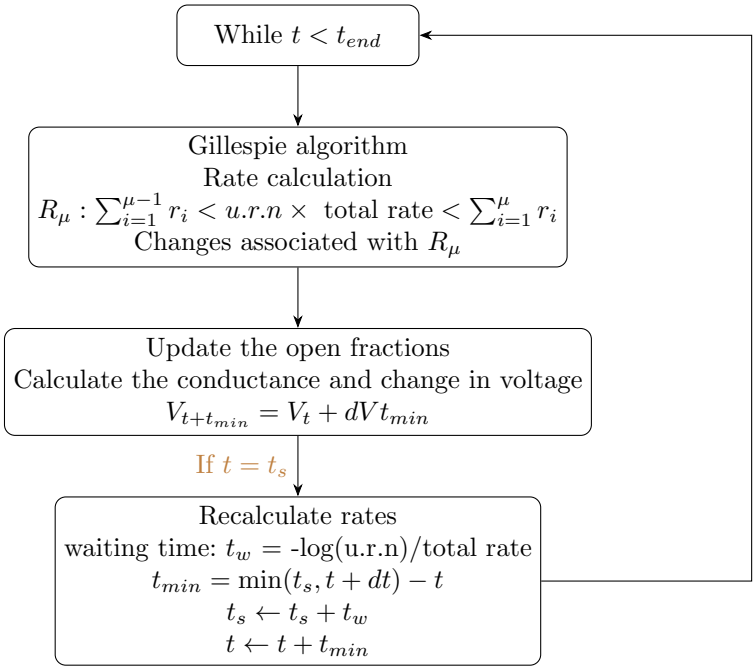
2.10 Analysis

To study the effect of various parameters on the switching dynamics, we look at the burst length and the switching frequency of the neurons, which is the primary functional read-out of the network.

Inter-spike interval and Firing frequency: The time difference between peaks

Algorithm 3 Tandem Progression Gillespie

$t_s \leftarrow$ time of the next transition,
$t_w \leftarrow$ time to the next transition,
$t \leftarrow$ current time,
$dt \leftarrow$ fixed time step,
$u.r.n \leftarrow$ uniform random number,
Initialize state vector for ion channels and rates.



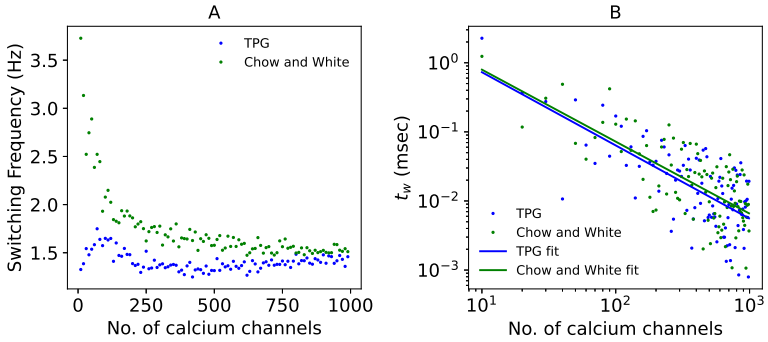


Fig. 1 Comparison of switching dynamics for TPG and algorithm used in [23] A. The mean switching frequency described by TPG, and, Gillespie implementation of Chow and White . B. The mean t_w (waiting time) for different numbers of calcium channel for the two algorithms.

of two consecutive action potentials is the inter-spike interval, and the inverse of the inter-spike interval gives us the firing frequency of the neuron.
Inter-burst interval and switching frequency: We define switching frequency as the frequency with which the neurons alternate in their activity. A burst is defined as a set of action potentials the neuron fires before the other neuron is released from inhibition and starts firing. When the burst terminates because of the sAHP current, and the other neuron takes over and inhibits the first neuron, the interval between the last action potential from the previous burst and the first action potential of the next burst of the neuron is called an inter-burst interval(IBI). The inverse of IBI is called switching frequency or burst frequency.

The action potential is detected if the voltage goes higher than 15 mV and if such a detection happens after a minimum time difference of 5 msec after the last detection. A burst is detected when inter-spike intervals are greater than twice the last inter-spike interval. We calculate the switching frequency by finding the inverse of the mean of a fixed number of burst lengths. As a measure of the regularity of bursts, the coefficient of variation is calculated, where T is the inter-burst interval, and is given by,

$$CV = \frac{\sqrt{\langle T^2 \rangle - \langle T \rangle^2}}{\langle T \rangle}$$

3 Results

3.1 Mechanism for rhythm generation

In the system described in Figure 2, switching occurs due to an action potential (AP) triggered build-up of a calcium-dependent potassium current, specifically called slow after-hyperpolarization (sAHP). The potassium current causes the neuronal membrane to be hyperpolarized. This hyperpolarization is long-lasting due to the intrinsic slow closing time of the sAHP channel, similar to what is seen in CA1 neurons in the hippocampus [27]. As the potassium current builds up, it makes it incrementally more difficult for the neuron to fire an AP in response to a stimulus (conductance of sAHP grows with every calcium spike that closely follows APs). Eventually, the action potentials shut down and deactivate the inhibitory synaptic current (GABAergic) to the connected neuron. This release from inhibition enables the other neuron to fire action potentials, creating the 121212 activity pattern.

A detailed chronology of events is as follows: Strong DC input is applied to both neurons (with identical intrinsic properties but slightly different initial conditions). Action potentials are generated in one of the neurons with advantageous initial conditions. The resulting synaptic current inhibits activity in the other neuron via a GABA synapse. In the active neuron, in the meantime, APs cause the opening of voltage-gated calcium channels (VGCCs). The opening and closing activity of VGCCs closely follows the open-close action of APs. The incoming calcium flux through VGCCS activates the sAHP channels (Figure 2 B, top three panels). sAHP channels respond rapidly to calcium. However, as the name suggests, sAHP channels inactivate slowly; therefore, with each calcium pulse, the number of active sAHP channels increases. The

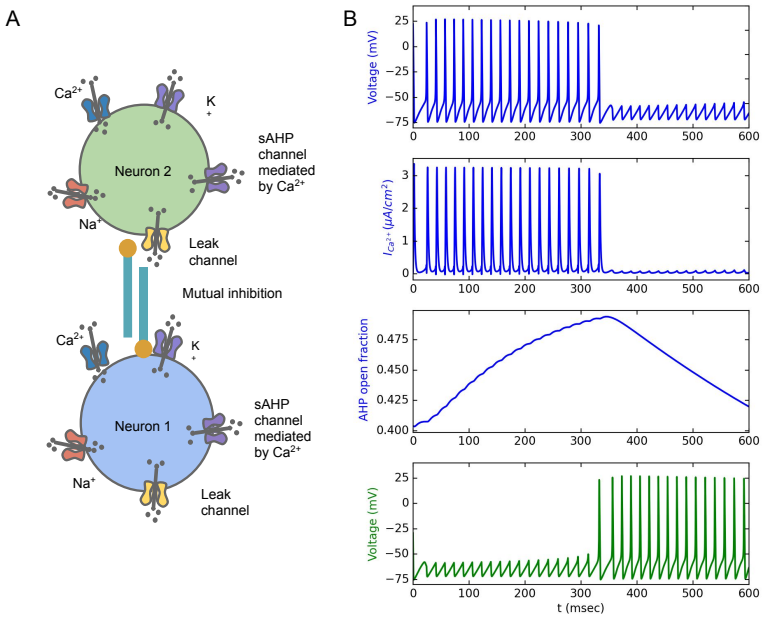


Fig. 2 Network and switching mechanism: A. The network of mutually inhibiting neurons, along with the ion channels which, orchestrate the firing and switching activity of the neurons. B. Top to bottom: Neuron fires action potentials due to depolarization driven by the external current. Calcium channels open as a result of depolarization of the membrane, leading to calcium ion influx. The build-up of sAHP current over multiple action potentials leads to the termination of burst in neuron 1. Escape from inhibition and burst of the neuron 2.

slow closing time of the channels allows them to remain open even after calcium channels are closed and calcium is extruded out, and also ensures that potassium builds over multiple action potentials. When the membrane is sufficiently hyperpolarized, induced by the potassium current, the neuron is hyperpolarized. Thus, the action of sAHP terminates the AP activity after a characteristic time interval governed by the potassium current build-up [28](Figure 2 B, third panel). The termination of the burst of APs puts an end to the active inhibitory synaptic current. The other neuron gets activated now and completes the rhythmic pattern (Figure 2 B bottom panel).

The total time taken for the activity to switch from one neuron to the other, the 'Inter-Burst-Interval' (see Methods), depends on the external current stimulus $I_{external}$, its influence on synaptic conductance, G_{syn}, the time constant of the synaptic current $\tau_{synapse}$, the conductance of the sAHP current g_{sAHP}, and the AHP-calcium-binding rates and extrinsic noise (Figure 2 A) (Figure 2 B third top panel). These contribute to the potassium current differentially and dictate the burst interval.

3.2 Modulation of switching frequency by driving current

For physiologically realistic synaptic coupling strengths and sAHP conductance (synaptic conductance $= 2.2mS/cm^2$, $g_{sahp} = 0.4mS/cm^2$) ([19]), the switching of

activity between neurons is modulated little over two Hz (0.8 Hz-3 Hz) for an external current between 13 $\mu A/cm^2$ to 18.75 $\mu A/cm^2$ (Figure 3 A). As the input current is increased further, the hyperpolarizing action of the SAHP is inadequate to terminate the firing, resulting in the cessation of the switching. The dependence of switching frequency on the external current can be summarized as follows: An increase in driving current makes both the neurons more excitable and leads to an increase in spiking frequency (Figure 3 B). This increase leads to an increased rate of calcium spikes and a faster build-up of sAHP current at high driving currents (Figure 3 C), which can shorten the duration over which the neuron is active (burst duration). On the other hand, the increase in depolarizing input drive also increases the hyperpolarization needed to terminate the burst via the sAHP current (expressed in terms of threshold sAHP open fraction) (Figure 3 D). This has the effect of increasing the duration of the burst, as it takes longer to reach the threshold sAHP current. The increase in the threshold of the sAHP current needed to terminate the burst is shown in Figure 3 D. These distinct opposite effects on the rate of sAHP built-up in response increase in the driving current are shown in Figure 3 C. Enhanced depolarization dictates the initial decrease in the rate of AHP build-up until I_{ext}=16 $\mu A/cm^2$. This is followed by an increase in the rate of sAHP build-up due to a faster rate of incoming calcium spikes. The spike frequency increases with an increase in driving current, causing a decrease in the switching frequency (from 13 $\mu A/cm^2$ to 16 $\mu A/cm^2$) (Figure 3 A). This can be explained by the time taken for sAHP to achieve higher conductance levels, thus extending the switching time. Between the input current 15 $\mu A/cm^2$ and 16 $\mu A/cm^2$, the frequency of switching remains around 0.8 Hz. However, beyond 16 $\mu A/cm^2$, the switching frequency increases as it follows the sAHP build-up rate. Increasing the external driving current to both the neurons described by I_{ext} in equation (1) (while keeping other parameters unchanged) thus has a non-monotonic effect on the switching frequency (Figure 3 A).

3.3 Modulation of switching frequency by extrinsic noise

To investigate the effect of extrinsic noise on the switching times between the two neurons, we simulate additive current noise ($\xi \in \mathcal{N}(0,1)$), equation (1)). Recall that regular switching is orchestrated by calcium current and the intrinsic opening and closing timescale of the sAHP current. At intermediate current values, a minimum in the coefficient of variation (CV) of switching response (Figure 4 A, blue) is observed that corresponds to a minimum in sAHP rate (Figure 4 A, green). This indicates that the network is most insensitive to external noise for a finite range of input currents. At these values of intermediate current, the sAHP current integrates noisy input current best to maintain regular switching. At high input current and the consequent stronger depolarization, the threshold AHP fraction needed to achieve termination of the burst is higher. High input thus makes the burst duration longer and leads to smoothing of the noisy input by the sAHP current. The filtering of noisy input is seen as a lower CV (see Figure 4 A, blue); the cumulative effect of the fluctuations is seen as an increased switching frequency. In sum, switching frequency is seen to increase with

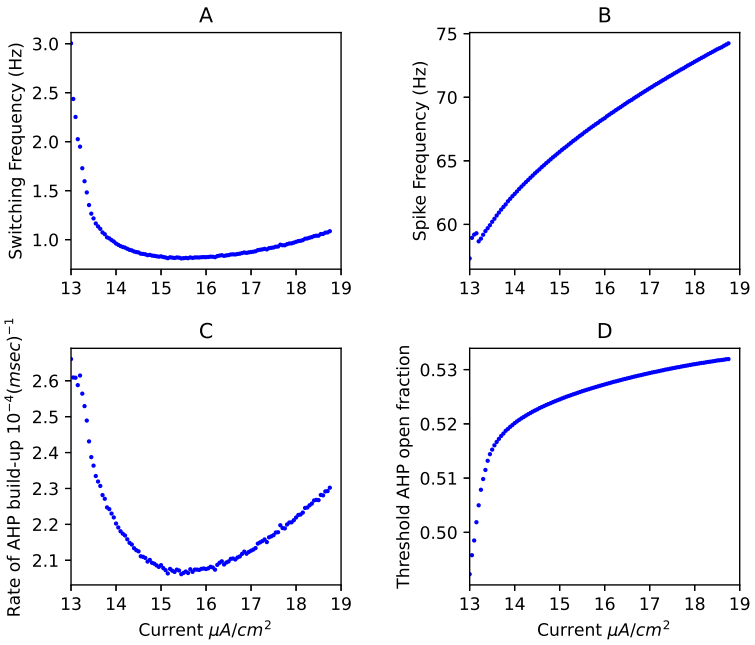


Fig. 3 Frequency modulation by current: Competition between increased excitability and sAHP threshold current leads to non-monotonic changes in switching frequency: A. The switching frequency shows a non-monotonic dependence on the external current due to two opposing effects that increasing current has on the neuron's excitability. B. The spike frequency increases with increasing current. C. The rate of build-up sAHP current shows a minimum at an intermediate current value. D. The peak sAHP open fraction increases monotonically with the increase in current.

noise amplitude(Figure 4 B, C (black), and D). The switching frequency for three illustrative current values as a function of noise amplitude is shown in Figure 4 D.

The role of sAHP current in increasing the switching frequency in response to noisy inputs can be understood in the following way: Current noise causes voltage fluctuations, leading to fluctuations in the voltage-gated calcium current. The sAHP current can note each of these fluctuations in calcium concentration due to its fast rise time. However, as the sAHP current's decay time is long, the rise in sAHP due to calcium fluctuations accumulates over time and leads to a quicker build-up of sAHP current (Figure 4 E, green). The faster build-up of sAHP terminates the burst earlier, increasing the switching frequency (Figure 4 C, black) with a minor increase in the CV of switching (Figure 4 C, blue). The stochastic calcium signal is filtered with a slow decay time of the sAHP current, and only the summation over time rather than the individual calcium fluctuations dictates the termination of the burst. In figure 4 F, the percentage change in switching frequency range (calculated as: $\frac{[f_{max}-f_{min}]_{\text{noise amp}}}{[f_{max}-f_{min}]_{\text{no noise}}} \times 100$) is shown. The addition of noise increases the range of switching frequencies achieved by $\sim$ 350 % at noise amplitude 1.5. In summary, reliable switching over a wider range of frequencies can be achieved by input noise due to the biophysical properties of the sAHP current.

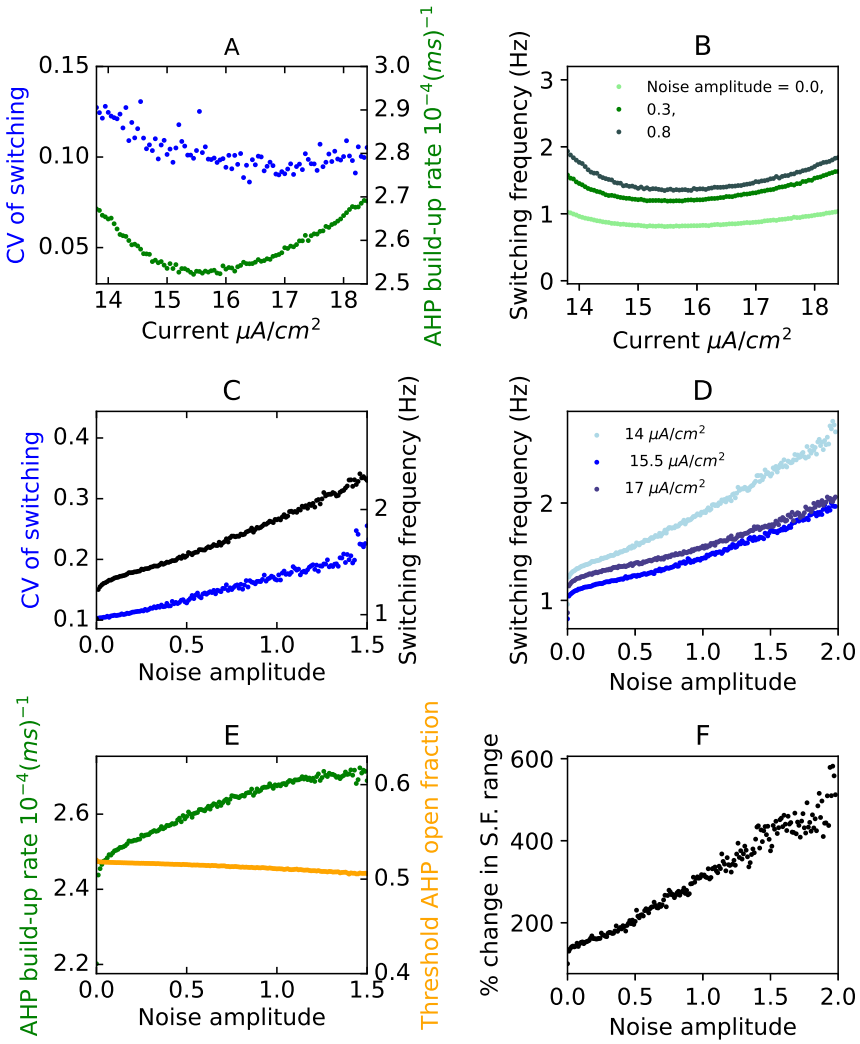


Fig. 4 Optimal excitability helps in maintaining reliable switching in the presence of extrinsic noise: A. The minimum in the sAHP build-up (green) rate corresponds to a minimum in the CV of switching (blue) for noise amplitude 0.8. B. The switching frequency increases by increasing the amplitude of the noise. C. The switching frequency (black) and the CV of switching (blue) increase on increasing the noise amplitude for current = $14\mu A/cm^2$. D. Switching frequency versus the noise amplitude for three driving current values. E. The rate of sAHP-build (green) increases as the noise amplitude is increased. In contrast, the threshold sAHP conductance (open fraction in yellow) remains almost constant on increasing the noise amplitude for current = $14\mu A/cm^2$. F. The switching frequency range increases by ~ 350 percent for current = $14\mu A/cm^2$ with the addition of noise along with some unreliability in switching (CV=0.2 at noise amplitude =1.5).

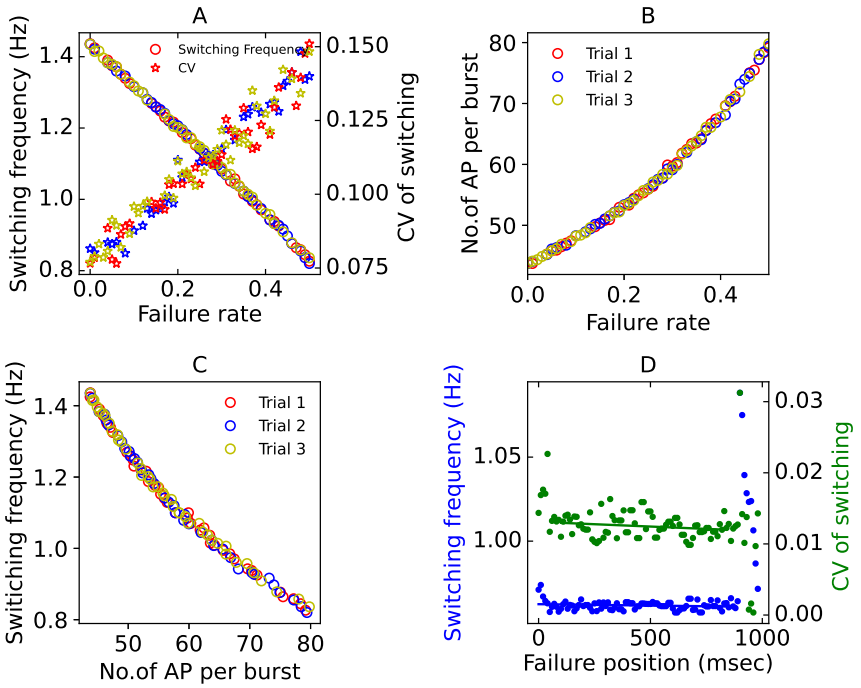


Fig. 5 Switching dynamics in the presence of calcium pulse failures. A. The mean switching frequency(circles) and CV of switching(stars) for three different trials of calcium pulse failures for a range of failure rates. B. Average number of action potentials in a burst as a function of failure rate. C. The Switching frequency is a function of failure rate and correlates negatively with the number of APs per burst. D. One single calcium pulse failure is induced, and the position of failure is varied during the burst (failure position zero indicates that the failure happened at the initiation of the burst, and failure position 1000 indicates that the failure happened after 1000 msec of the burst initiation). Switching frequency (blue) and CV (green) of switching as a function of failure position.

3.4 Modulation by intrinsic noise: effect of calcium pulse failures on switching dynamics

To further examine the sensitivity of sAHP response to the fluctuations in calcium current, we introduce random calcium pulse failures at varying rates. Increasing the rate of calcium pulse failure decreased the switching frequency (Figure 5 A) due to a slower build-up of sAHP current (an increasing number of calcium pulses are missed by sAHP current). Predictably, the increase in the failure rate has the effect of increasing the CV of switching (Figure 5 A). In the presence of a "stochastically faulty" calcium pulse generator, more action potentials need to be fired by the neuron to achieve the threshold sAHP current to terminate the burst. We show that the increase in the failure rate (probability) leads to an increase in the number of action potentials per burst (Figure 5 B). More action potentials are needed to achieve burst termination, which also makes the burst longer. Thus, the switching frequency decreases with the increase in the number of action potentials in the burst (Figure 5 C). A linear decrease in switching frequency with increasing the failure rate (Figure 5 A) is seen. Interestingly,

similar trends are seen for independent random trials of the calcium pulse failures occurring randomly during the epoch of the burst. The invariance to the temporal position of missed calcium pulses during the burst indicates that the switching behavior is dictated by the number of calcium pulses causing the build of sAHP current and is insensitive to the temporal order of these calcium pulses.

To systematically test the insensitivity of the sAHP current to the temporal characteristic of the stimulus train, we induced one failure per burst. We changed the temporal position of the calcium pulse failure relative to the initiation of the burst. We see that the position of the failure does not affect the switching frequency for most of the burst and only affects it towards the end of the burst above 900 msec in failure position (Figure 5 D, blue). The failure at the end of the burst has a drastic effect on the switching frequency. At the end of the burst, the depolarization is weak, and the inhibition from the inhibiting neuron is strong. Thus, missing a calcium pulse close to the termination of the burst reduces the depolarizing current in the neuron. In the meantime, the other neuron takes over and inhibits the neuron whose burst is about to end. This results in increased switching frequency when calcium failures appear at the end of the burst (Figure 5 D, blue). A missed calcium pulse here also increases irregularity in switching (Figure 5 D, green). However, the CV of the switching remains the same for most missed temporal positions of the calcium pulse. This is illustrated in Figure 5 D, green. In summary, the sAHP current serves as an action potential counter and makes the neuron insensitive to the variations in temporal patterns of the stimulus for a fixed level of noise.

3.5 Modulation of switching frequency by calcium channel noise

The stochastic opening of calcium channels is the most significant contributor to the variability in synaptic release [17]. To isolate the effect of calcium channel stochasticity on switching, Markovian opening and closing of channels were simulated; however, the rest of the system equations were simulated deterministically. Recall that our two-neuron system has intrinsic timescales that vary over a wide range (over two orders of magnitude $\tau_{sAHP} = 1.5sec, \tau_{cal} = 14msec$ [20]). The extant algorithms for Markovian simulations, Gillespie-like algorithms [9, 23], introduce errors that accumulate with time due to the intrinsic differences in timescales. We, therefore, developed an updating system for variables that we call the Tandem Progression Gillespie or TPG algorithm (See methods for details). According to TPG, 1) transitions in the calcium channel opening get updated according to the Gillespie algorithm, and 2) the deterministic changes in the rest of the variables (activation and inactivation gates of the ion channels) get updated according to an Euler integrator. Thus, by updating the whole system together at a time that arises either from the calcium channel fluctuations or the voltage equations, the dynamics of this multi-timescale system evolved more accurately. This method is in line with the simulation of Piecewise-Deterministic Markov Processes [29].

We see that the switching frequency follows a non-monotonic trend with increasing the number of VGCCs (Figure 6 A). The CV of switching decreases with increasing

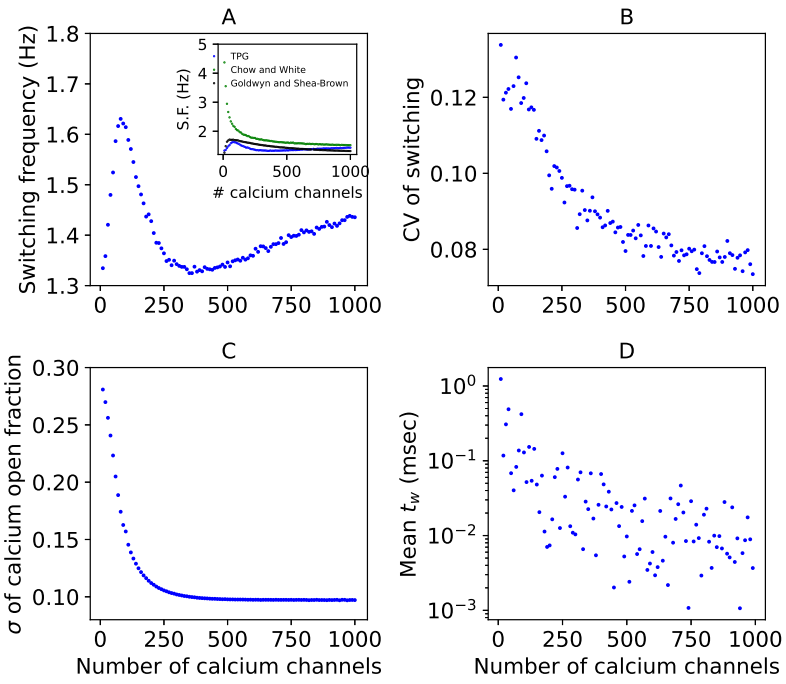


Fig. 6 The opposite effects of increasing the number of channels lead to non-monotonic variation in switching frequency. A: The switching frequency shows a non-monotonic trend with increasing the number of calcium channels. B. The switching becomes more regular as the amplitude of fluctuations decreases with the increase in the number of calcium channels. C. The fluctuations in the open fraction of calcium channels become smaller in amplitude with the increasing channel number. D. The mean transition time in the calcium channel states decreases as channel number is increased, leading to increased frequency of fluctuations in calcium concentration.

channel numbers (Figure 6 B) as the fluctuations in open fraction become smaller in amplitude when the number of calcium channels is increased (Figure 6 C). Beyond about 100 VGCCS, the switching frequency decreases as the number of VGCCs is increased. The waiting times from the Gillespie algorithm become shorter as the number of VGCCs is increased (Figure 6 D). When the number of VGCCs is further increased, beyond 400 VGCCs, the fluctuations become smaller in amplitude, but their frequency increases (Compare Figure 6 C and D). Due to the slow timescales of the sAHP current, these closely spaced fluctuations add up in the sAHP current and thus maintain a 'memory' of these fluctuations. This build-up of sAHP current results in an increase in switching frequencies at large numbers of VGCCs. Thus, increasing the calcium channel numbers causes 1) a decrease in the amplitude of fluctuations and 2) an increase in the frequency of fluctuations, which have opposing effects on the switching frequency. The two opposing effects cause the non-monotonic trend to be observed in the switching frequency upon increasing the number of calcium channels. These simulations are carried out for the same maximum conductance of the calcium current.

4 Discussion

It is conjectured that the brain is fundamentally a rhythm-generating machine [30]. All functions of the brain, from motor patterns and breathing to cognition, emerge from various rhythms. Reciprocal inhibition between neuron pairs is 'the' building block that generates stable antiphasic and multiphasic output patterns. The switching in these reciprocally inhibited networks occurs due to either intrinsic biophysical properties of ionic currents that assign a distinct periodicity to the rhythm or an external drive. There is a distinct advantage in studying these systems: The relative simplicity of these building block circuits can make it easier to investigate the basic principles of rhythm generation. Thus, experimental intervention can be carried out in these isolated small circuits to gain insights into how networks of neurons generate behavior.

We have capitalized on this simplest network capable of rich dynamical behavior. We investigate how intrinsic and extrinsic noise affect the regularity of the switching of activity in two mutually inhibiting neurons. Switching in our model takes place due to the calcium-mediated potassium current (sAHP) build-up. The sAHP current allows one neuron to 'escape from inhibition' of the other [31]. Previous studies have investigated the role of noise in modulating neuronal firing rates [13, 21, 32–34]. Current noise either reduces or enhances the gain of the firing frequency–current relationship depending on the type of intrinsic currents associated with the cell [35]. Noise is also seen to induce higher switching frequencies in CPGs of the rat spinal cord [36]. Some of the other consequences of extrinsic factors on the switching frequency of two mutually inhibiting neurons are described by Skinner et al.[37]. Our results demonstrate the non-monotonic effect of increasing external current on switching frequency. The initial decrease followed by the increase in switching frequency occurs because of the competing impact of increasing the external current (Figure 3), faster build-up of the sAHP current, and a higher threshold acquired to escape from inhibition. Neuromodulators can modulate biophysical properties such as the channel conductance and calcium-binding rates [38] and can further modulate the range of switching repertoire of the network. It would be interesting to study how slow time scales of activation associated with neuromodulation further affect the network rhythm [39].

We describe the effect of varying the amplitude of current noise (Figure 4) on the switching dynamics. We show that the switching frequency repertoire of the network is extended when current noise is introduced in the simulations (Figure 4). An analytical description of this phenomenon that uses a phenomenological neuron (Fitzhugh-Nagumo neuron) as an oscillatory system with multiple separable timescales appears in Nesse et al. 2008 [34]. We find that this noise-induced enhancement of the dynamical range of switching takes place at a small cost of an increase in variability. The CV of switching is also seen to depend on the amplitude of the external current stimulus (Figure 4C, A, and D). Reliable switching in the presence of noise over a range of driving current suggests a match between the calcium spike frequencies driven by the current stimulus and the timescale of sAHP over which sAHP integrates the current fluctuations. A similar mechanism via a match in timescales of fluctuations and sAHP current could explain the regular switching seen in many systems such as the Lamprey locomotion CPG and pre-Botzinger complex [7, 33, 40]. It may not

always be possible to update a biological system's intrinsic parameters in an activity-dependent manner. Here, we show that external noise can be advantageous rather than a hindrance and extend the neuron's dynamic range.

We examined the effect of calcium channel fluctuations, the most significant intrinsic noise source in neurons [17]. Forcing random failures in calcium spikes leads to the linear dependence of switching frequency on the failure rate (Figure 5). We also show that the rate of switching is invariant over multiple trials, i.e., the switching frequency is insensitive to the position of failure of the calcium spike. This invariability over numerous trials demonstrates that sAHP current is a spike counter and can serve as a temporal integrator. Temporal integration has been implicated in audio and visual systems and involves collating spike patterns over time to improve detection or discrimination [41]. A reliable temporal integrator must sustain a consistent average rhythm despite any disruptions or variations in the input signals. The network with sAHP current can serve that purpose. A slow afterhyperpolarization that rises from Na^{+1}/K^{+1} pump dynamics can also act as an integrator of spike number and serve as cellular memory on the time scales of the cycle periods of the locomotion rhythms [42]. Separately, potassium current with slow inactivation has been implicated in modulating synaptic plasticity and short-term memory by changing the excitability of the cell [43–45]. It would be interesting to investigate if sAHP dynamics simulated in our network would give rise to some form of cellular, short-term memory.

The opening of calcium channels is rapid and closely follows the action-potential activity. However, as mentioned before, the response of the calcium-mediated potassium current, sAHP, is much slower (by one order of magnitude). Thus, each action potential leads to a fractional increase in the conductivity of these channels. The firing ceases as the potassium current builds up over a train of action potentials. To account for fast calcium channel stochasticity and the slow cumulative increase in sAHP, we modified the classical Gillespie algorithm [22]. We believe that the modified algorithm, TPG, captures the fluctuations and progressions governing the neuronal and network dynamics over multiple timescales more accurately.

We also investigated the effect of varying calcium channel numbers while keeping the maximum conductance the same on the network's switching dynamics (Figure 6). As expected, the CV of switching decreases as the channel number increases. However, the switching frequency has a non-monotonic dependence on the number of calcium channels. An upstroke in switching frequency is seen for a range of ion channel numbers ($\sim$ 10 - 50). The larger fluctuations in the fraction of open channels result in this behavior. As the open channel numbers fluctuate widely, the network has more significant excursions through switching intervals dictated by the open fraction. In contrast, when a small number of calcium channels are present, the waiting times for transitions between states of calcium channels are too long, and higher frequencies of switching are not achieved (Figure 6 D). Interestingly, the number of channels that orchestrate the highest switching frequencies ($\sim$ 50 - 100) is also a realistic estimate for the number of L-type calcium channels present in the neuron [17]. An increasing trend in switching frequency is seen again for large numbers of ion channels ($>$ 400). It is noteworthy that the switching frequency at these high channel numbers (Figure 6 A for current = $14\mu A/cm^2$) is larger than the deterministic limit of switching frequency

(Figure 3 D for current = $14\mu A/cm^2$). The small waiting times due to the large population statistics of calcium channels (Figure 6 D) lead to frequent fluctuations in the calcium current. A corollary insight from these calculations is that stochasticity also plays a role when channel numbers are large and slow dynamics are involved, in contrast to the conventional belief. In sum, the competing effects of fluctuations and waiting times for calcium channels to change states lead to the non-monotonic behavior seen in switching frequency as we vary the number of calcium channels (Figure 6 A).

The brain is capable of generating regular firing patterns critical for several functions despite irregular inputs due to channel fluctuations, probabilistic neurotransmitter release, diffusion of signaling molecules, probabilistic binding to receptors, etc. It is almost impossible to suppress all sources of noise experimentally. Computational modeling to isolate the consequences of noise on function is therefore valuable. Using a minimalistic model system for rhythm generation, our investigations have led to several novel insights into the contribution of noise to function. Each calcium fluctuation may not immediately affect the postsynaptic neuron; however, an ionic current like sAHP seems to keep an account of this miniature activity. We speculate that this may serve as a sub-cellular mechanism to retain an extended account of neuronal activity ([42]).

Acknowledgements

We would like to thank Dr. Collins Assisi for useful insights and past and present members of Nadkarni and Assisi labs for helpful discussions.

Declarations

- Funding: Suhita Nadkarni (SN): Wellcome Trust/DBT India Alliance (grant number IA/I/12/1/500529). Subhadra Mokashe (SM) : Department of Science and Technology (DST), Government of India - Innovation in Science Pursuit for Inspired Research (INSPIRE) –DST/INSPIRE Fellowship, Indian Institute of Science Education and Research, Pune, and Wellcome Trust/DBT India Alliance (grant number IA/I/12/1/500529) and Science & Engineering Research Board, India (grant number PDF/2017/001803).
- Conflict of interest/Competing interests: The authors declare that the research was conducted in the absence of any commercial or financial relationships that could be construed as a potential conflict of interest.
- Ethics approval and consent to participate: Not applicable
- Consent for publication: Not applicable
- Data availability: Not applicable
- Materials availability: Not applicable
- Code availability: Code will be made available upon publication.
- Author contribution: SN conceived the project. SN and SM designed the model simulations. SM ran the simulations. SM and SN analyzed the data. SM and SN wrote the manuscript.

References

[1] Pelkey, K.A., Chittajallu, R., Craig, M.T., Tricoire, L., Wester, J.C., McBain, C.J.: Hippocampal GABAergic Inhibitory Interneurons. Physiological reviews **97**(4), 1619–1747 (2017) https://doi.org/10.1152/physrev.00007.2017

[2] Otto Friesen, W.: Reciprocal inhibition: A mechanism underlying oscillatory animal movements. Neuroscience and Biobehavioral Reviews **18**(4), 547–553 (1994) https://doi.org/10.1016/0149-7634(94)90010-8

[3] Daun, S., Rubin, J.E., Rybak, I.A.: Control of oscillation periods and phase durations in half-center central pattern generators: A comparative mechanistic analysis. Journal of Computational Neuroscience **27**(1), 3–36 (2009) https://doi.org/10.1007/s10827-008-0124-4

[4] Lu, J., Sherman, D., Devor, M., Saper, C.B.: A putative flip-flop switch for control of REM sleep. Nature **441**(7093), 589–94 (2006) https://doi.org/10.1038/nature04767

[5] Myre, C.D., Woodward, D.J.: Bistability, switches and working memory in a two-neuron inhibitory-feedback model. Biological Cybernetics **68**(5), 441–449 (1993) https://doi.org/10.1007/BF00198776

[6] Hooper, S., Moulins, M.: Switching of a neuron from one network to another by sensory-induced changes in membrane properties. Science **244**(4912), 1587–1589 (1989) https://doi.org/10.1126/science.2740903 https://science.sciencemag.org/content/244/4912/1587.full.pdf

[7] Cangiano, L., Grillner, S.: Mechanisms of rhythm generation in the lamprey locomotor network. PhD thesis, Karolinska Institute (2004)

[8] Dragoi, G., Buzsáki, G.: Temporal encoding of place sequences by hippocampal cell assemblies. Neuron **50**(1), 145–157 (2006) https://doi.org/10.1016/j.neuron.2006.02.023

[9] Goldwyn, J.H., Shea-Brown, E.: The what and where of adding channel noise to the Hodgkin-Huxley equations. PLoS Computational Biology **7**(11) (2011) https://doi.org/10.1371/journal.pcbi.1002247 arXiv:1104.4823

[10] Faisal, A.A., Selen, L.P.J., Wolpert, D.M.: Noise in the nervous system. Nature Reviews Neuroscience **9**(4), 292–303 (2008) https://doi.org/10.1038/nrn2258

[11] Stacey, W.C., Durand, D.M.: Synaptic noise improves detection of subthreshold signals in hippocampal ca1 neurons. Journal of Neurophysiology **86**(3), 1104–1112 (2001) https://doi.org/10.1152/jn.2001.86.3.1104 https://doi.org/10.1152/jn.2001.86.3.1104. PMID: 11535661

[12] McDonnell, M.D., Abbott, D.: What is stochastic resonance? Definitions, misconceptions, debates, and its relevance to biology. PLoS Computational Biology **5**(5) (2009) https://doi.org/10.1371/journal.pcbi.1000348

[13] Schmid, G., Goychuk, I., Hänggi, P.: Stochastic resonance as a collective property of ion channel assemblies. Europhysics Letters (EPL) **56**(1), 22–28 (2001) https://doi.org/10.1209/epl/i2001-00482-6 arXiv:0106036 [physics]

[14] Andreev, A.V., Makarov, V.V., Runnova, A.E., Pisarchik, A.N., Hramov, A.E.: Coherence resonance in stimulated neuronal network. Chaos, Solitons & Fractals **106**, 80–85 (2018) https://doi.org/10.1016/j.chaos.2017.11.017

[15] White, J.A., Rubinstein, J.T., Kay, A.R.: Channel noise in neurons. Trends in Neurosciences **23**(3), 131–137 (2000) https://doi.org/10.1016/S0166-2236(99)01521-0

[16] Tegnér, J., Hellgren-Kotaleski, J., Lansner, A., Grillner, S.: Low-voltage-activated calcium channels in the lamprey locomotor network: simulation and experiment. Journal of neurophysiology **77**(4), 1795–1812 (1997)

[17] Modchang, C., Nadkarni, S., Bartol, T.M., Triampo, W., Sejnowski, T.J., Levine, H., Rappel, W.-J.: A comparison of deterministic and stochastic simulations of neuronal vesicle release models. Physical biology **7**(2), 026008 (2010) https://doi.org/10.1088/1478-3975/7/2/026008

[18] Hodgkin, A.L., Huxley, A.F.: A quantitative description of membrane current and its application to conduction and excitation in nerve. Bulletin of Mathematical Biology **52**(1-2), 25–71 (1990) https://doi.org/10.1007/BF02459568 arXiv:NIHMS150003

[19] Sah, P., Clements, J.D.: Photolytic manipulation of [Ca2+]i reveals slow kinetics of potassium channels underlying the afterhyperpolarization in hippocampal pyramidal neurons. The Journal of neuroscience : the official journal of the Society for Neuroscience **19**(10), 3657–3664 (1999)

[20] Stanley, D.A., Bardakjian, B.L., Spano, M.L., Ditto, W.L.: Stochastic amplification of calcium-activated potassium currents in Ca 2+ microdomains. Journal of Computational Neuroscience **31**(3), 647–666 (2011) https://doi.org/10.1007/s10827-011-0328-x

[21] Wang, X.-J.: Calcium coding and adaptive temporal computation in cortical pyramidal neurons. J Neurophysiol **79**(3), 1549–1566 (1998) https://doi.org/10.1152/jn.1998.79.3.1549

[22] Gillespie, D.T.: A general method for numerically simulating the stochastic time evolution of coupled chemical reactions. Journal of Computational Physics **22**(4), 403–434 (1976) https://doi.org/10.1016/0021-9991(76)90041-3

[23] Chow, C.C., White, J.a.: Spontaneous action potentials due to channel fluctuations. Biophysical journal **71**(6), 3013–3021 (1996) https://doi.org/10.1016/S0006-3495(96)79494-8

[24] Ankri, N., Debanne, D.: A fast markovian method for modeling channel noise in neurons. Heliyon **9**(6) (2023) https://doi.org/10.1016/j.heliyon.2023.e16953

[25] Stubenrauch, J., Auer, N., Kempter, R., Lindner, B.: Stochastic synaptic dynamics under learning. PRX Life **4**, 023006 (2026) https://doi.org/10.1103/r21z-29nv

[26] Camassa, A., Galluzzi, A., Mattia, M., Sanchez-Vives, M.V.: Deterministic and stochastic components of cortical down states: Dynamics and modulation. Journal of Neuroscience **42**(50), 9387–9400 (2022) https://doi.org/10.1523/JNEUROSCI.0914-22.2022 https://www.jneurosci.org/content/42/50/9387.full.pdf

[27] Sahu, G., Turner, R.W.: The molecular basis for the calcium-dependent slow afterhyperpolarization in ca1 hippocampal pyramidal neurons. Frontiers in Physiology **Volume 12 - 2021** (2021) https://doi.org/10.3389/fphys.2021.759707

[28] Manira, A., Tegner, J., Grillner, S., Manira, A.E.L.: Calcium-dependent potassium channels play a critical role for burst termination in the locomotor network in lamprey. Journal of Neurophysiology **72**(4), 1852–1861 (1994)

[29] Davis, M.H.A.: Piecewise-deterministic markov processes: A general class of nondiffusion stochastic models. Journal of the Royal Statistical Society. Series B (Methodological) **46**(3), 353–388 (1984)

[30] Buzsáki, G.: Rhythms of the Brain, p. 464. Oxford University Press, New York (2006). https://doi.org/10.1093/acprof:oso/9780195301069.001.0001

[31] Wang, X., Rinzel, J.: Alternating and synchronous rhythms in reciprocally inhibitory model neurons. Neural Computation **4**(1), 84–97 (1992) https://doi.org/10.1162/neco.1992.4.1.84

[32] Morozova, E., Newstein, P., Marder, E.: Reciprocally inhibitory circuits operating with distinct mechanisms are differently robust to perturbation and modulation. eLife **11**, 74363 (2022) https://doi.org/10.7554/eLife.74363

[33] Nesse, W.H., Del Negro, C.A., Bressloff, P.C.: Oscillation regularity in noise-driven excitable systems with multi-time-scale adaptation. Physical Review Letters **101**(8), 3–6 (2008) https://doi.org/10.1103/PhysRevLett.101.088101

[34] Nesse, W.H., Borisyuk, A., Bressloff, P.C.: Fluctuation-driven rhythmogenesis in an excitatory neuronal network with slow adaptation. Journal of Computational Neuroscience **25**(2), 317–333 (2008) https://doi.org/10.1007/s10827-008-0081-y

[35] Higgs, M.H., Slee, S.J., Spain, W.J.: Diversity of gain modulation by noise in neocortical neurons: Regulation by the slow afterhyperpolarization conductance. Journal of Neuroscience **26**(34), 8787–8799 (2006) https://doi.org/10.1523/JNEUROSCI.1792-06.2006 https://www.jneurosci.org/content/26/34/8787.full.pdf

[36] Taccola, G.: The locomotor central pattern generator of the rat spinal cord in vitro is optimally activated by noisy dorsal root waveforms. Journal of neurophysiology **106**(2), 872–84 (2011) https://doi.org/10.1152/jn.00170.2011

[37] Skinner, F.K., Kopell, N., Marder, E.: Mechanisms for oscillation and frequency control in reciprocally inhibitory model neural networks. Journal of Computational Neuroscience **1**(1-2), 69–87 (1994) https://doi.org/10.1007/BF00962719

[38] Schwartz, E.J., Gerachshenko, T., Alford, S.: 5-HT prolongs ventral root bursting via presynaptic inhibition of synaptic activity during fictive locomotion in lamprey. Journal of neurophysiology **93**(2), 980–8 (2005) https://doi.org/10.1152/jn.00669.2004

[39] Kozlov, A., Kotaleski, J.H., Aurell, E., Grillner, S., Lansner, A.: Modeling of substance P and 5-HT induced synaptic plasticity in the lamprey spinal CPG: Consequences for network pattern generation. Journal of Computational Neuroscience **11**(2), 183–200 (2001) https://doi.org/10.1023/A:1012806018730

[40] Rancic, V., Gosgnach, S.: Recent insights into the rhythmogenic core of the locomotor cpg. International Journal of Molecular Sciences **22**(3) (2021) https://doi.org/10.3390/ijms22031394

[41] Saija, J.D., Başkent, D., Andringa, T.C., Akyürek, E.G.: Visual and auditory temporal integration in healthy younger and older adults. Psychological Research **83**(5), 951–967 (2019) https://doi.org/10.1007/s00426-017-0912-4

[42] Pulver, S.R., Griffith, L.C.: Spike integration and cellular memory in a rhythmic network from Na+/K+ pump current dynamics. Nature Neuroscience **13**(1), 53–59 (2010) https://doi.org/10.1038/nn.2444

[43] Turrigiano, G.G., Marder, E., Abbott, L.F.: Cellular short-term memory from a slow potassium conductance. Journal of neurophysiology **75**(2), 963–6 (1996)

[44] Marder, E., Abbott, L.F., Turrigiano, G.G., Liu, Z., Golowasch, J.: Memory from the dynamics of intrinsic membrane currents. Proceedings of the National Academy of Sciences of the United States of America **93**(24), 13481–13486 (1996) https://doi.org/10.1073/pnas.93.24.13481

[45] Stackman, R.W., Hammond, R.S., Linardatos, E., Gerlach, A., Maylie, J., Adelman, J.P., Tzounopoulos, T.: Small conductance Ca2+-activated K+ channels modulate synaptic plasticity and memory encoding. Journal of neuroscience

22(23), 10163–10171 (2002)